

Accurate exchange-correlation energies for the warm dense electron gas

Fionn D. Malone,^{1,*} N. S. Blunt,² Ethan W. Brown,³ D.K.K. Lee,¹
J.S. Spencer,^{1,4} W.M.C. Foulkes,¹ and James J. Shepherd^{5,1}

¹*Department of Physics, Imperial College London,
Exhibition Road, London SW7 2AZ, United Kingdom.*

²*University Chemical Laboratory, Cambridge University,
Lensfield Road, Cambridge CB2 1EW, United Kingdom.*

³*Institute for Theoretical Physics, ETH Zürich, Wolfgang Pauli Strasse 27, 8093 Zürich, Switzerland.*

⁴*Department of Materials, Imperial College London,
Exhibition Road, London SW7 2AZ, United Kingdom.*

⁵*Department of Chemistry, Massachusetts Institute of Technology,
Cambridge, MA, 02139, United States of America.*

(Dated: February 12, 2019)

Density matrix quantum Monte Carlo is used to sample exact-on-average N -body density matrices for uniform electron gas systems of up to 10^{124} matrix elements via a stochastic solution of the Bloch equation. The results of these calculations resolve a current debate over the exchange-correlation energies necessary for the parametrization of finite-temperature density functionals. Exchange-correlation energies calculated using the real-space restricted path-integral formalism and the k -space configuration path-integral formalism disagree by up to $\sim 10\%$ at certain reduced temperatures $T/T_F < 0.5$ and densities $r_s \leq 1$. We are able to verify the exact-in-principle configuration path-integral Monte Carlo numbers at high density and bridge the gap between high and low densities.

The accurate simulation of correlated electrons in matter under extreme conditions has recently become a topic of intense interest [1] due to their importance to inertial confinement fusion [2], the constitution of planetary interiors [3] and the laser irradiation of solids [4]. Simulations offer a powerful adjunct in the interpretation of often difficult experiments in these regimes. The high electronic temperatures encountered in warm dense environments require electronic structure techniques able to capture accurately the quantum mechanical, thermal, many-body, and material effects.

Density functional theory (DFT) offers a good compromise between accuracy and efficiency in electronic structure theory. Almost all modern density functionals are based on a parametrization of the exchange-correlation energy of the uniform electron gas (UEG) as a function of density at zero temperature [5–8]. This is insufficient in the warm dense regime, where a parametrization of the exchange-correlation free energy over the whole temperature-density plane is required [9–11]. A significant step towards providing this much needed data was achieved by Brown *et al.* [12] using the restricted path-integral Monte Carlo (RPIMC) method, with local density parametrizations quickly following [13–15]. However, soon after this, an alternative technique, configuration path-integral Monte Carlo (CPIMC), was applied to the same problem and gave substantially different results.

This Letter resolves the disagreement between the two path-integral methods. We describe an alternative approach, density matrix quantum Monte Carlo (DMQMC) [16, 17], which is, in principle, exact in a given basis set at any temperature or density. By introducing a systematically improvable approximation analogous to the initiator approximation of full configuration-interaction quantum Monte Carlo (FCIQMC) [18, 19], we show that

DMQMC can be made capable of treating system sizes comparable to those tackled using RPIMC. We then use initiator DMQMC to settle the controversy and provide data which can be corrected to the thermodynamic limit using existing techniques [12, 15].

Warm dense electrons.— The UEG can be described by the dimensionless density parameter $r_s = \tilde{r}_s/a_0$, where a_0 is the Bohr radius and \tilde{r}_s is the Wigner-Seitz radius, and by the dimensionless temperature $\Theta = T/T_F$, with T_F being the Fermi temperature of a three-dimensional free electron gas of the same density. In the warm dense regime, $r_s \approx \Theta \approx 1$, perturbative methods [20–22] fail due to the lack of any small coupling parameter, and numerical techniques such as QMC are required.

Real-space RPIMC is regarded as the state-of-the-art method for simulating thermal effects in materials [23]. Very recently, however, Schoof *et al.* performed highly accurate simulations using the k -space CPIMC method [24, 25] and obtained results in substantial disagreement with RPIMC for the internal energy of the spin-polarized UEG in the high density and low temperature regime [26]. The same group has also reported disagreements with RPIMC at higher temperatures and lower densities, this time by comparing with the direct [27] and permutation blocking [28] path-integral (PB-PIMC) approaches. Groth, Dornheim and coworkers [29, 30] have applied CPIMC and PB-PIMC to the polarized and unpolarized UEG across the entire density range for temperatures above $\Theta = 0.5$, finding better agreement with RPIMC for the unpolarized UEG than for the polarized UEG. These disagreements will have to be resolved before finite-temperature DFT can be used with the same degree of confidence as its ground-state counterpart.

The DMQMC method.— The exact, equilibrium, properties of any quantum system can be derived from

the canonical N -particle density matrix

$$\hat{\rho} = e^{-\beta\hat{H}}, \quad (1)$$

with $\beta = 1/k_B T$ and the normalization given by the partition function

$$Z = \text{Tr } \hat{\rho}. \quad (2)$$

Typically, these equations are tackled using path-integral Monte Carlo methods [24, 31], where Eq. (2) is written as a sum over paths in imaginary time and the paths are sampled using Metropolis Monte Carlo [32].

In contrast, in DMQMC, we solve for the (modified) density matrix [33]

$$\hat{f}(\tau) = e^{-\frac{1}{2}(\beta-\tau)\hat{H}^0} e^{-\tau\hat{H}} e^{-\frac{1}{2}(\beta-\tau)\hat{H}^0}, \quad (3)$$

via the Bloch-like equation

$$\frac{d\hat{f}}{d\tau} = \frac{1}{2}\{\hat{H}^0, \hat{f}\} - \frac{1}{2}\left(\hat{H}_I(-\alpha)\hat{f} + \hat{f}\hat{H}_I(\alpha)\right), \quad (4)$$

where $\{\cdot, \cdot\}$ is the usual anti-commutator [34], we have partitioned the Hamiltonian as $\hat{H} = \hat{H}^0 + \hat{H}'$, and $\hat{H}_I(\alpha)$ is the interaction-picture Hamiltonian defined as

$$\hat{H}_I(\alpha) = e^{\alpha\hat{H}^0} \hat{H}' e^{-\alpha\hat{H}^0}, \quad (5)$$

for $\alpha = \frac{1}{2}(\beta-\tau)$. Typically, \hat{H}^0 is chosen to be the kinetic energy operator or the diagonal of the Hamiltonian. Note that $\hat{f}(\tau=0) = e^{-\beta\hat{H}^0}$ and $\hat{f}(\tau=\beta) = \hat{\rho}$.

A deterministic evaluation of $\hat{\rho}$ is intractable for all but the smallest systems – the storage of the matrix alone rapidly overwhelms even the most modern of computers. Instead, we seek a stochastic approach. Inspired by the FCIQMC method [18], we solve Eq. (4) using a collection of signed walkers to represent the elements of the density matrix $f_{ij} = \langle D_i | \hat{f} | D_j \rangle$, where $|D_i\rangle$ and $|D_j\rangle$ are members of a set of orthonormal many-particle basis states. In this work, the basis states are Slater determinants of plane waves. A simulation proceeds by evolving an initial distribution of walkers at $\tau=0$, chosen to provide an unbiased statistical sample of the initial density matrix $e^{-\beta\hat{H}^0}$, using a population dynamics algorithm derived from a simple Euler approximation to Eq. (4) [16, 17]. During one time step $\Delta\tau$, a walker on density matrix element f_{ij} spawns a child at f_{ik} with probability

$$p_s(\mathbf{ij} \rightarrow \mathbf{ik}) \propto \frac{\Delta\tau}{2} |\tilde{H}_{jk}| e^{-\alpha(E_k^0 - E_j^0)}, \quad (6)$$

where $E_j^0 = \langle D_j | \hat{H}^0 | D_j \rangle$ and $\tilde{H}_{jk} = (H_{jk} - S\delta_{jk})$, with S an adjustable shift parameter used to control the total population of walkers N_w [18, 35]. The sign of the child is $\text{sign}(-\tilde{H}_{jk})$ times the sign of the parent. A similar expression determines the spawning probability $p(\mathbf{ij} \rightarrow \mathbf{kj})$ along columns of the density matrix. The walker on element f_{ij} is then allowed to die or clone (reproduce)

with probability $p_d(\mathbf{ij}) \propto \frac{\Delta\tau}{2} |(H_{ii}^0 - \tilde{H}_{ii}) + (H_{jj}^0 - \tilde{H}_{jj})|$. Cloning occurs if $(H_{ii}^0 - \tilde{H}_{ii}) + (H_{jj}^0 - \tilde{H}_{jj}) > 0$, with death in the opposite case. Finally, walkers of opposite sign on the same element are annihilated and removed from the simulation.

The sign problem in path-integral methods is characterized by an exponential decrease in the average sign with increased system size and decreased temperature. In FCIQMC and DMQMC, by contrast, an exponentially increasing number of walkers is required for the ground state to emerge from the noise. The critical number of walkers depends on the annihilation rate, which is much enhanced in a discrete Hilbert space [18, 36, 37]. In practice, the critical population is small enough to allow DMQMC to sample the N -particle density matrix *exactly* for system sizes far outside the reach of conventional diagonalization. The availability of the full density matrix allows arbitrary expectation values to be evaluated without uncontrolled approximations, whether or not the operator of interest commutes with the Hamiltonian [16].

Basis sets.– For the UEG we choose the many-particle states to be Slater determinants of plane waves, $\psi_{\mathbf{k}\sigma}(\mathbf{r}) = \frac{1}{\sqrt{\Omega}} e^{i\mathbf{k}\cdot\mathbf{r}}$, where σ is the electron spin, $\mathbf{k} = \frac{2\pi}{L}(n, m, l)$ with $n, m, l \in \mathbb{Z}$, and $\Omega = L^3$ is the simulation cell volume. The dimension of the Hilbert space is restricted by imposing a spherical kinetic energy cutoff $\varepsilon_c = \frac{1}{2}k_c^2$, ensuring that the single-particle basis contains a finite number M of plane waves. The density matrix is sampled in the corresponding space of $\left(\sum_{\zeta} \binom{M}{N_{\uparrow}} \binom{M}{N_{\downarrow}}\right)^2$ antisymmetrized tensor products of plane waves (Slater determinants), where $\zeta = (N_{\uparrow} - N_{\downarrow})/N$ is the spin polarization, N_{\uparrow} and N_{\downarrow} are the numbers of spin-up and spin-down electrons, and $N = N_{\uparrow} + N_{\downarrow}$.

At zero temperature, convergence to the complete basis set ($M \rightarrow \infty$) limit is required for an accurate description of electron-electron cusps in the many-electron wavefunction. In the large M limit, the internal energy converges like M^{-1} for $\zeta = 0$ and $M^{-5/3}$ for $\zeta = 1$ [38–42]. Matters are somewhat complicated at finite temperatures due to the competing convergence of the electron-electron cusp in the potential energy ($V = \langle \hat{V} \rangle \equiv Z^{-1} \text{Tr}[\hat{V}\hat{\rho}]$) and the contribution of highly energetic single-particle states to the kinetic energy ($T = \langle \hat{T} \rangle$) [17]. Figure 1 shows, however, that for $N = 33$, $\zeta = 1$, and $\Theta = 0.5$, the convergence is rapid, with any remaining basis set error being less than 1 milli-Hartree per particle when $M = 1237$. Differences between results for larger values of M lie within the stochastic error bars.

Initiator Approximation.– The critical populations necessary to overcome the sign problem at low temperatures are too large for most systems of interest and approximations are therefore required. We use an analogue of the initiator approximation developed for the FCIMQC method (*i*-FCIQMC) [19], which has been used in a variety of successful chemical [45–47], model [39, 40] and solid-state FCIQMC simulations [48] and has been

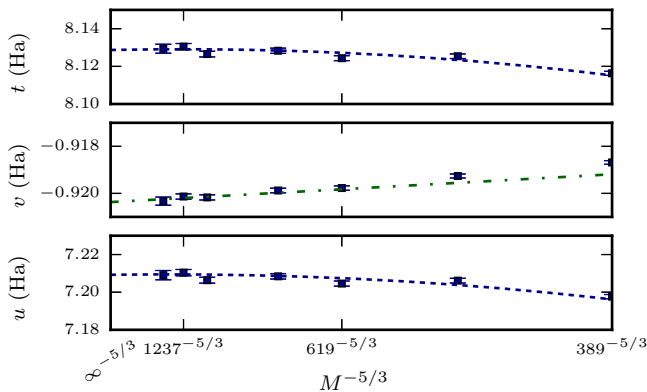


FIG. 1. Convergence of various contributions to the internal energy ($u = U/N$) as a function of basis set for $N = 33$, $r_s = 0.6$, $N_w = 10^5$ and $\Theta = 0.5$ calculated using i -DMQMC. We see the $M^{-5/3}$ cusp-like convergence in the potential energy per particle ($v = V/N$), while the kinetic energy per particle ($t = T/N$) saturates past $M \approx 619$ plane waves. The internal energy per particle slightly decreases as M increases beyond this value. The green dot-dashed line is a weighted least-squares fit [43] to the last 4 points in v assuming an $M^{-5/3}$ dependence, while the dashed blue lines are cubic fits to the data [44].

applied to UEG systems of up to 54 unpolarized electrons at zero temperature [39, 40]. While spawning to already-occupied determinants is unaffected, the initiator approximation only allows spawning events to unoccupied determinants that originate from a set of ‘initiator determinants’ with walker populations above a certain adjustable threshold, n_{add} , or that result from multiple sign-coherent spawning events from non-initiator determinants. Here we find it equally useful at finite temperature. The effects of the initiator approximation may be reduced by increasing the total walker population, N_w , with the original DMQMC algorithm recovered as $N_w \rightarrow \infty$.

In DMQMC, due to the sparse sampling of the initial condition, we find that a direct application of the initiator approximation can lead to incorrect averages at higher temperatures. This happens when the i -DMQMC algorithm has too little imaginary time to determine the initiator space dynamically. While the results should still be valid in the $N_w \rightarrow \infty$ limit, the rate of convergence to this limit can be slow. To ameliorate this problem, we permanently set all density matrix elements at excitation levels $n_{\text{ex}} \leq 2$ to be initiators. (A density matrix element at excitation level n_{ex} is one for which the bra and the ket differ by n_{ex} particle-hole pairs.) This reduces the effect of the initiator approximation in the early stages of the simulation, before the initiator distribution has been properly determined. At lower temperatures, this modification becomes less important as the initial walker population occupies a relatively small number of low-energy diagonal density matrix elements. The effects of intro-

N_w	r_s		
	0.6	1	2
1×10^4	3.8894(2)	1.1458(2)	0.12491(5)
1×10^5	3.8899(1)	1.1460(2)	0.12423(9)
1×10^6	3.8893(2)	1.1455(2)	0.12223(7)
5×10^6	3.8893(2)	1.1452(2)	0.1211(5)

TABLE I. Convergence of the i -DMQMC internal energy per particle with the target walker number, N_w , for $\Theta = 0.0625$, $N = 33$ and $M = 1045$ at a variety of r_s values with $n_{\text{add}} = 3$. For $r_s = 2$ we used $n_{\text{ex}} = 0$ and grew the population past $N_w = 10^5$, whilst for $r_s = 0.6, 1$ we used $n_{\text{ex}} = 2$ and kept the population fixed at N_w . The initiator error is typically smaller than 1 milli-Hartree per particle at $N_w > 10^6$.

ducing a permanent initiator space can be monitored by ensuring that the results do not change significantly as its size is increased.

In Table I we demonstrate the convergence as a function of N_w of the initiator error in the i -DMQMC estimate of the internal energy of a 33-electron, spin-polarised system with $r_s = 0.6, 1, 2$ and $\Theta = 0.0625$. Any bias is essentially negligible (estimated at less than 1%) for $N_w > 10^6$ and much smaller than $k_B T$. Similar convergence is found at higher temperatures [49], although the relative error is typically smaller which is to be expected as the sign problem is less severe.

Energies of the warm dense gas.— We are now in a position to provide results for $N = 33$, $\zeta = 1$, which has emerged as the standard benchmark system for the warm dense electron gas [12, 26, 28, 29]. We focus on the region $0.6 \leq r_s \leq 2$ and $0.0625 \leq \Theta \leq 0.5$, where the differences between the RPIMC and CPIMC results are largest [26]. All of the results presented have been carefully checked for convergence with respect to initiator and basis-set errors, and we believe them to be accurate to within the stochastic error bars. Precise values of M , N_w and the time step, $\Delta\tau$, along with the full i -DMQMC data set are available in the supplementary material [49]. Calculations were performed using the HANDE code [50] and used real amplitudes to improve the stochastic efficiency [51, 52]. We set $n_{\text{add}} = 3$ for all simulations. In most simulations we initialised the density matrix with N_w walkers and allowed the shift to vary throughout the simulation. For higher densities and the largest walker numbers we instead grew the population to its target value [49]. Results were averaged over between 20 and a few thousand independent runs depending on the target population and temperature considered. We found it efficient to revert to the original asymmetric formulation of DMQMC [17] for $\Theta \leq 0.125$ due to the potentially large weights appearing in the spawning probabilities (see Eq. (6)). However, both approaches produce statistically identical results [49].

The i -DMQMC results for the exchange-correlation energy per particle presented in Fig. 2 are in very good agreement with the CPIMC results at all values of r_s up

to the maximum of $r_s = 1$ considered by Schoof *et al.* [26]. The agreement is even better at lower r_s values. In particular, our results confirm that the kink-potential approximation used by Schoof [26] for $r_s \geq 0.6$ is well controlled and that the RPIMC results are significantly too low at $r_s = 1$. Our additional points in the range $1 \leq r_s \leq 2$ further suggest that the RPIMC results remain unreliable for all $r_s \leq 4$. We find a slight, apparently systematic, disagreement with CPIMC at $\Theta = 0.5$, although all points remain within error bars. The origin of this discrepancy is unknown but could be due to a failure of the initiator approximation used in DMQMC at high temperatures. This will be addressed in future work.

As further confirmation of the accuracy of our results, we have carried out independent *i*-FCIQMC calculations [49] of the internal energy at zero temperature. Assuming that the energy varies like T^2 for small T , we can extrapolate the *i*-DMQMC and RPIMC results to zero temperature and compare them with the *i*-FCIQMC data. Figure 3 shows that the extrapolated *i*-DMQMC energy agrees with the *i*-FCIQMC result, but that the extrapolated RPIMC energy is too low. This is in contrast to the seemingly reliable extrapolation of the size-corrected RPIMC data performed in [12], which agreed well with the Perdew-Zunger parametrization of the local density approximation [7]. Also plotted in Fig. 3 are two different finite-temperature mean-field estimates of the internal energy evaluated in the canonical ensemble (see caption for details), which are seen to perform relatively well.

Discussion & conclusion.— This paper introduced a systematically improvable approximation to DMQMC, allowing for significantly larger systems to be treated, and used it to study warm dense electron gases with up to 33 electrons. Remarkably, even though the largest density matrix sampled has approximately 10^{124} elements, we require as few as 10^5 walkers for certain densities.

Focusing on the canonical test system of $N = 33$ spin-polarized particles, we found excellent agreement between *i*-DMQMC and CPIMC for $r_s \leq 1$ and confirmed that the RPIMC results of [12] are unreliable at high densities. In the intermediate to low density regime, we observed significant but decreasing discrepancies persisting up to $r_s \approx 4$ and $\Theta \leq 0.5$, consistent with the results of Dornheim *et al.* [28]. Our results bridge the gap between the low- and high-density limits and can be used to aid in the parametrization of exchange-correlation functionals for finite-temperature DFT.

Our finite-system-size, ground-state and mean-field calculations confirm that that RPIMC internal energies are systematically too low even at low temperatures. This is inconsistent with the conventional view that the internal energy ought to be variational as $T \rightarrow 0$. These results are significant because RPIMC with free particle nodes is often considered the most accurate and consistent method available to study real warm dense matter systems [2, 23]. Our findings, when combined with the

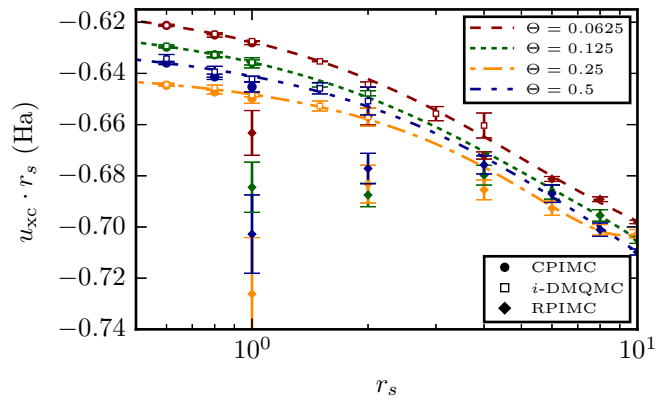


FIG. 2. Exchange-correlation energy per particle (times r_s) as a function of r_s , showing excellent agreement between *i*-DMQMC and CPIMC for $r_s \leq 1$ and differences between *i*-DMQMC and RPIMC for $1 \leq r_s \leq 4$. For the UEG, $u_{xc} = (U - U_0)/N$, where U_0 is the internal energy of the $N = 33$ non-interacting electron gas in the canonical ensemble. Lines are weighted third-order polynomial interpolations [44] between the *i*-DMQMC data and the RPIMC data for $r_s > 4$ and are meant as guides to the eye. The *i*-DMQMC results at $r_s = 3$ and $r_s = 4$ were obtained by performing a basis set extrapolation. The error bars here include an estimate for remaining initiator and basis set error [49].

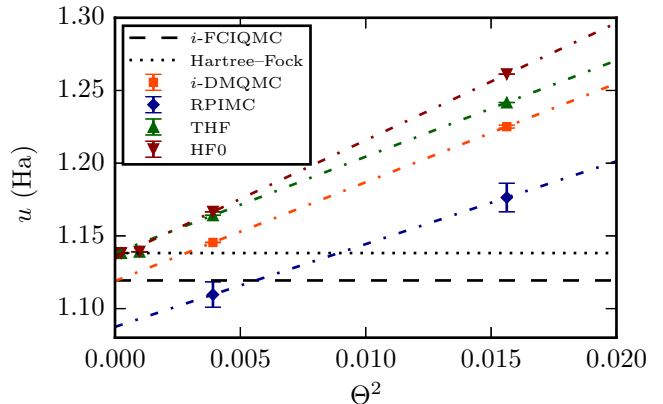


FIG. 3. Extrapolation [43] of the internal energy to $\Theta = 0$ for the $N = 33$, $\zeta = 1$, $r_s = 1$ system. The RPIMC energies are systematically too low and extrapolate to a value considerably below the *i*-FCIQMC ground-state energy. This discrepancy cannot be explained by finite-size effects. The *i*-DMQMC (and by extension CPIMC) results fare significantly better. Also shown are two mean-field estimates of the internal energy in the canonical ensemble. The first of these, $U_{\text{HF}0} = \langle \hat{H} \rangle_0$ with $\hat{\rho}_0 = e^{-\beta \hat{T}}$, incorporates the first order exchange contribution only; the second is defined by $U_{\text{THF}} = \langle \hat{H} \rangle_{\text{THF}}$ with $\hat{\rho}_{\text{THF}} = \sum_i e^{-\beta E_i^{\text{HF}}} |D_i\rangle \langle D_i|$ and $E_i^{\text{HF}} = \langle D_i | \hat{H} | D_i \rangle$. Note that $\hat{\rho}_{\text{THF}}$ is not the usual thermal Hartree-Fock density matrix [53] as the many-body eigenvalues appearing in the Boltzmann weights are independent of temperature. Both estimates can be evaluated using a Monte Carlo routine outlined in [17] and implemented in HANDE [50].

results of CPIMC and PB-PIMC simulations [26, 28–30], suggest that the free-particle nodal constraint may incur an error of 5-10%, depending on the density and observable considered. We believe that exponentially scaling, systematically exact methods such as *i*-DMQMC could be of use in analyzing and improving approximations made in RPIMC.

The *i*-DMQMC method is complementary to the CPIMC, PIMC (direct or restricted) and other novel path-integral [54] or finite-temperature FCIQMC approaches [55] and is particularly useful at low temperatures, where annihilation and the initiator approximation allow us to overcome the sign problem for surprisingly large systems in many cases [56]. Open technical challenges remain in the treatment of unpolarized systems and the development of reliable finite-size corrections at high temperature and density (see, e.g., the discussion in [26]), but we are confident that *i*-DMQMC will have an important role to play in the eventual complete characterization of the warm dense electron gas. Finally, given that *i*-DMQMC only requires access to Hamiltonian ma-

trix elements and samples the full density matrix, it may provide exciting opportunities to investigate the thermodynamics of real warm dense matter exactly.

Acknowledgements.— We thank Tim Schoof and Michael Bonitz for helpful discussions facilitated by a CECAM workshop, and for providing unpublished data at early stages of this research. FDM is funded by an Imperial College PhD Scholarship. NSB acknowledges Trinity College, Cambridge for funding. JJS thanks the Royal Commission for the Exhibition of 1851 for a Research Fellowship. FDM, JSS and WMCF acknowledge the research environment provided by the Thomas Young Centre under Grant No. TYC-101. WMCF received support from the UK Engineering and Physical Sciences Research Council under grant EP/K038141/1. Computing facilities were provided by the High Performance Computing Service of Imperial College London, by the Swiss National Supercomputing Centre (CSCS) under project ID s523, and by ARCHER, the UK National Supercomputing Service, under EPSRC grant EP/K038141/1 and via a RAP award.

-
- * Author to whom correspondence should be addressed. Electronic mail: f.malone13@imperial.ac.uk
- [1] F. Graziani, *Frontiers and Challenges in Warm Dense Matter*, Vol. 96 (Springer Science & Business, 2014).
- [2] S. X. Hu, B. Militzer, V. N. Goncharov, and S. Skupsky, *Phys. Rev. B* **84**, 224109 (2011).
- [3] J. J. Fortney, S. H. Glenzer, M. Koenig, B. Militzer, D. Saumon, and D. Valencia, *Phys. Plasmas* **16**, 041003 (2009).
- [4] R. Ernstorfer, M. Harb, C. T. Hebeisen, G. Sciaini, T. Dartigalongue, and R. J. D. Miller, *Science* **323**, 1033 (2009).
- [5] D. M. Ceperley and B. J. Alder, *Phys. Rev. Lett.* **45**, 566 (1980).
- [6] S. H. Vosko, L. Wilk, and M. Nusair, *Can. J. Phys.* **58**, 1200 (1980).
- [7] J. P. Perdew and A. Zunger, *Phys. Rev. B* **23**, 5048 (1981).
- [8] J. P. Perdew and Y. Wang, *Phys. Rev. B* **45**, 13244 (1992).
- [9] N. D. Mermin, *Phys. Rev.* **137**, A1441 (1965).
- [10] E. Brown, *Path integral Monte Carlo and the electron gas*, Ph.D. thesis, University of Illinois at Urbana-Champaign (2014).
- [11] V. V. Karasiev, L. Calderín, and S. Trickey, *arXiv preprint arXiv:1601.04543* (2016).
- [12] E. W. Brown, B. K. Clark, J. L. DuBois, and D. M. Ceperley, *Phys. Rev. Lett.* **110**, 146405 (2013).
- [13] E. W. Brown, J. L. DuBois, M. Holzmann, and D. M. Ceperley, *Phys. Rev. B* **88**, 081102 (2013).
- [14] T. Sjöström and J. Dufty, *Phys. Rev. B* **88**, 115123 (2013).
- [15] V. V. Karasiev, T. Sjöström, J. Dufty, and S. B. Trickey, *Phys. Rev. Lett.* **112**, 076403 (2014).
- [16] N. S. Blunt, T. W. Rogers, J. S. Spencer, and W. M. C. Foulkes, *Phys. Rev. B* **89**, 245124 (2014).
- [17] F. D. Malone, N. S. Blunt, J. J. Shepherd, D. K. K. Lee, J. S. Spencer, and W. M. C. Foulkes, *J. Chem. Phys.* **143**, 044116 (2015).
- [18] G. H. Booth, A. J. W. Thom, and A. Alavi, *J. Chem. Phys.* **131**, 054106 (2009).
- [19] D. Cleland, G. H. Booth, and A. Alavi, *J. Chem. Phys.* **132**, 041103 (2010).
- [20] F. Perrot and M. W. C. Dharma-wardana, *Phys. Rev. A* **30**, 2619 (1984).
- [21] W.-D. Kraeft, D. Kremp, W. Ebeling, and G. Röpke, *Quantum statistics of charged particle systems* (Springer, 1986).
- [22] J. Vorberger, M. Schlanges, and W. D. Kraeft, *Phys. Rev. E* **69**, 046407 (2004).
- [23] B. Militzer and K. P. Driver, *Phys. Rev. Lett.* **115**, 176403 (2015).
- [24] T. Schoof, M. Bonitz, A. Filinov, D. Hochstuhl, and J. W. Dufty, *Contr. Plasma Phys.* **51**, 687 (2011).
- [25] T. Schoof, S. Groth, and M. Bonitz, *Contr. Plasma Phys.* **55**, 136 (2015).
- [26] T. Schoof, S. Groth, J. Vorberger, and M. Bonitz, *Phys. Rev. Lett.* **115**, 130402 (2015).
- [27] V. S. Filinov, V. E. Fortov, M. Bonitz, and Z. Moldabekov, *Phys. Rev. E* **91**, 033108 (2015).
- [28] T. Dornheim, T. Schoof, S. Groth, A. Filinov, and M. Bonitz, *J. Chem. Phys.* **143**, 204101 (2015).
- [29] S. Groth, T. Schoof, T. Dornheim, and M. Bonitz, *Phys. Rev. B* **93**, 085102 (2016).
- [30] T. Dornheim, S. Groth, T. Schoof, C. Hann, and M. Bonitz, *arXiv preprint arXiv:1601.04977* (2016).
- [31] D. M. Ceperley, *Rev. Mod. Phys.* **67**, 279 (1995).
- [32] N. Metropolis, A. W. Rosenbluth, M. N. Rosenbluth, A. H. Teller, and E. Teller, *J. Chem. Phys.* **21**, 1087 (1953).
- [33] We use the interaction-picture version of DMQMC [17] but symmetrize the equations of motion. This allows ex-

- pectation values of operators that do not commute with the Hamiltonian to be evaluated accurately at low temperatures. The quality of estimates of expectation values of operators that commute with the Hamiltonian is unaffected [49].
- [34] $\{A, B\} = AB + BA$.
- [35] C. J. Umrigar, M. P. Nightingale, and K. J. Runge, *J. Chem. Phys.* **99**, 2865 (1993).
- [36] J. S. Spencer, N. S. Blunt, and W. M. C. Foulkes, *J. Chem. Phys.* **136**, 054110 (2012).
- [37] M. H. Kolodrubetz, J. S. Spencer, B. K. Clark, and W. M. C. Foulkes, *J. Chem. Phys.* **138** (2013).
- [38] A. Gulans, *J. Chem. Phys.* **141**, 164127 (2014).
- [39] J. J. Shepherd, G. Booth, A. Grüneis, and A. Alavi, *Phys. Rev. B* **85**, 081103 (2012).
- [40] J. J. Shepherd, G. H. Booth, and A. Alavi, *J. Chem. Phys.* **136**, 244101 (2012).
- [41] J. J. Shepherd, A. Grüneis, G. H. Booth, G. Kresse, and A. Alavi, *Phys. Rev. B* **86**, 035111 (2012).
- [42] J. Klimeš, M. Kaltak, and G. Kresse, *Phys. Rev. B* **90**, 075125 (2014).
- [43] E. Jones, T. Oliphant, P. Peterson, *et al.*, (2001–), [Online; accessed 2016-02-10].
- [44] S. Van Der Walt, S. C. Colbert, and G. Varoquaux, *Comput. Sci. & Eng.* **13**, 22 (2011).
- [45] G. H. Booth, D. Cleland, A. J. Thom, and A. Alavi, *J. Chem. Phys.* **135**, 084104 (2011).
- [46] D. Cleland, G. H. Booth, C. Overy, and A. Alavi, *J. Chem. Theory Comput.* **8**, 4138 (2012).
- [47] R. E. Thomas, G. H. Booth, and A. Alavi, *Phys. Rev. Lett.* **114**, 033001 (2015).
- [48] G. H. Booth, A. Grüneis, G. Kresse, and A. Alavi, *Nature* **493**, 365 (2013).
- [49] See supplementary material at [URL to be inserted by journal] for the full QMC data set as well as results at further temperatures and r_s values.
- [50] See <http://www.hande.org.uk/> for details on how to acquire the source code.
- [51] F. R. Petruzielo, A. A. Holmes, H. J. Changlani, M. P. Nightingale, and C. J. Umrigar, *Phys. Rev. Lett.* **109**, 230201 (2012).
- [52] N. S. Blunt, S. D. Smart, J. A. F. Kersten, J. S. Spencer, G. H. Booth, and A. Alavi, *J. Chem. Phys.* **142**, 184107 (2015).
- [53] N. D. Mermin, *Ann. Phys.* **21**, 99 (1963).
- [54] T. Dornheim, S. Groth, A. Filinov, and M. Bonitz, *New J. of Phys.* **17**, 73017 (2015).
- [55] N. S. Blunt, A. Alavi, and G. H. Booth, *Phys. Rev. Lett.* **115**, 050603 (2015).
- [56] A systematic study of the range of applicability of i -DMQMC is left for future work.